Journal of the European Ceramic Society 13 (1994) 239–246

Improvement of Oxidation Behaviour of Dense Silicon Nitride by Surface Modification

Chr. Taut, M. Herrmann

Fraunhofer Einrichtung für Keramische Technologien und Sinterwerkstoffe (IKTS) Winterbergstraße 28, D-01277 Dresden, Germany

G. Große

IFW Dresden, Winterbergstraße 28, D-01277 Dresden, Germany

P. Thiele

FTE Humboldt Universität Berlin, Invalidenstraße 110, D-10115 Berlin, Germany

&

Y. Gogotsi

Tokyo Institute of Technology, Research Laboratory of Engineering Materials, Center for Ceramics Research, 4259 Nagatsuta, Midori-ku, Yokohama 227, Japan

(Received 27 May 1993; revised version received 26 October 1993; accepted 12 November 1993)

Abstract

The effect of surface modifications by ion assisted deposition of platinum layers on the oxidation behaviour of dense silicon nitride was examined. Gas pressure sintered silicon nitride containing neodymia or yttria and alumina as sintering aids was coated with up to 1.5 μm Pt by magnetron sputtering. The morphology, residual stresses, chemical composition and crystal parameters of the coatings were characterized by SEM, XRD and electron beam microanalysis. The oxidation behaviour was investigated at 1100 °C, 1300 °C and 1450 °C in flowing air. In comparison with uncoated surfaces the Pt coated surfaces were, after oxidation, less damaged by cracking, bubbles formation and spalling. The oxidation reaction was masked by the decomposition of platinum oxide and crystallization processes. Experimental results indicate that the observed improvement of oxidation resistance of the investigated materials is caused by the change of the composition and properties of the growing oxide layers, by the change of diffusion- and oxidation - processes and by promotion of the selective crystallization of silicates in the oxide layer.

Es wurden die Auswirkungen der Oberflächenmodifizierung durch ionengestütztes Beschichten mit Platin auf das Oxidationsverhalten dichter Siliziumnitridkeramik untersucht. Druckgesintertes Siliziumnitrid mit Neodym- bzw. Yttrium- und Aluminiumoxid als Sinterhilfsmittel wurde mit ≤ 1.5 μm Pt durch Magnetronsputtern beschichtet. Morphologie, Eigenspannungszustand, chemische Zusammensetzung und Gitterparameter der Sputterschichten wurden mikroskopisch, durch Rontgenbeugungs- und Ionenstrahl-Mikroanalyse charakterisiert. Das Oxidationsverhalten wurde bei 1100 °C, 1300 °C und 1450 °C durch Auslagerung in Luft untersucht. Die Oxidschichten Pt gesputterter Oberflächen waren nach der Oxidation stärker und feiner kristallisiert und deutlich weniger durch Riß- und Blasenbildung sowie Abplatzungen geschädigt, als unbeschichtete Oberflächen. Die Oxidationsreaktion war durch Kristallisationsprozesse und die Zersetzung von PtO_2 überlagert. Die experimentellen Ergebnisse zeigen, daß die beobachtete Verbesserung des Hochtemperatur-Oxidationsverhaltens der untersuchten Siliziumnitridmaterialien auf einer Veränderung von Zusammensetzung und Eigenschaften der entstehenden Oxidschichten, einer veränderten Diffusions- bzw. Oxidationscharakteristik und der Förderung selektiver Kristallisationsprozesse in den Oxidschichten beruht.

On a étudiée l'influence d'un traitement en surface par déposition ionique de platine sur l'oxydation d'un nitrure de silicium dense. Par pulvérisation magnétron, on a recouvert un nitrure de silicium fritté sous pression, contenant des additifs de frittage tels que de

Journal of the European Ceramic Society 0955-2219/94/$7.00

l'oxyde de néodyme, d'yttrium, ou de l'alumine, par une couche de Pt pouvant atteindre 1,5 µm d'épaisseur. On a caractérisé la morphologie, les contraintes résiduelles, la composition chimique et les paramètres cristallins du revêtement par MEB, diffraction X et à la microsonde de Castaing. On a étudié l'oxydation sous air à 1100 °C, 1300 °C et 1450 °C. Comparées aux surfaces non traitées, les surfaces recouvertes de Pt se sont révélées, après oxydation, moins fissurées, écaillées, endommagées par la formation de cavités. La réaction d'oxydation est masquée par une décomposition de l'oxyde de platine, suivie de processus de cristallisation. Les résultats expérimentaux indiquent que l'amélioration observée de la résistance à l'oxydation des matériaux étudiés provient d'un changement dans la composition et les propriétés des couches d'oxyde qui se forment, d'une modification des processus de diffusion—et d'oxydation—et du fait que la cristallisation de silicates dans la couche d'oxyde est favorisée.

1 Introduction

The densification of nonoxide ceramics with predominantly covalent bonding character requires the presence of a liquid phase during sintering. After sintering it exists as a glassy or partially crystallized 'grain boundary phase'. This phase plays a crucial role in the oxidation processes. There are different methods for the improvement of the oxidation resistance of silicon nitride ceramics:

- —Crystallization of grain boundary phases,
- – modification of the composition of the grain boundary phase for the purpose of promoting the crystallization of the phases, which are in the thermodynamic equilibrium with SiO_2 and Si_3N_4:
- —surface modification of the ceramic with the purpose of
  - —eliminating surface flaws,
  - creating protecting layers.

The manufacturing of such layers on the surface of monoxide ceramics is known by chemical vapour deposition (for instance, CVD Si_3N_4 and SiC layers on the surfaces of porous RBSN ceramic[1]). Major disadvantages of this process are the high deposition temperatures and residual stresses, leading to the cracking and spalling of coatings. Methods using ion beams for surface modification, like ion implantation, ion-beam sputtering and ion beam mixing, have recently been developed.[2] Ion implantation processes reach only a depth of some nm, while the ion-beam sputtering methods allow deposition rates up to 100 nm/s.[3] These techniques have many advantages, viz. slight temperature exposition of the specimen, high density, good adhesion, purity and stability of the coating, and they allow desirable compositions with gradients of concentration and properties to be produced.

The purpose of the present work was either to build a diffusion barrier or to modify the ceramic surface in such a way, that the growing surface oxide layer gets an improved passivating character and therefore leads to a longer lifetime and/or a higher working temperature of the ceramic. The oxidation behaviour of dense, sintered silicon nitride (SSN) with magnetron sputtered Pt coatings of a thickness up to 1.5 µm was investigated.

2 Experimental

Dense SSN bars with alumina and yttria or neodymia additives were prepared by gas pressure sintering (1850 °C, 5 MPa N_2, 1.5 h)[4]. Their composition and properties are presented in Table 1. In material A (Si_3N_4 with Y_2O_3 and Al_2O_3 as sintering aids), apart from β-Si_3N_4, traces of melilite ($Y_2Si_3O_3N_4$?) were found (Fig. 1). A little amorphous halo is caused by the glassy part of the grain boundary phase. No secondary crystalline phases were detected in material B (Si_3N_4 with neodymia and alumina as sintering aids).

The specimens were ultrasonically cleaned in trichloroethylene and alcohol and dried (90 °C, 30 min) before sputtering. Pt was magnetron sputtered on the surfaces (working pressure: 0.8 Pa Ar, energy: 100 W (material A)/250 W (material B); target: Pt) by the Institute of Electron Physics at the Humboldt University, Berlin. Material A was coated with Pt layers of 405 nm, 810 nm and 1500 nm and material B with 650 nm and 1000 nm thick Pt layers. The bulk material and surface layers were investigated by surface roughness measurements, electron beam microanalysis and X ray diffraction (XRD). The σ- and texture analyses were carried out on a horizontal diffractometer with ψ,ϕ goniometer.

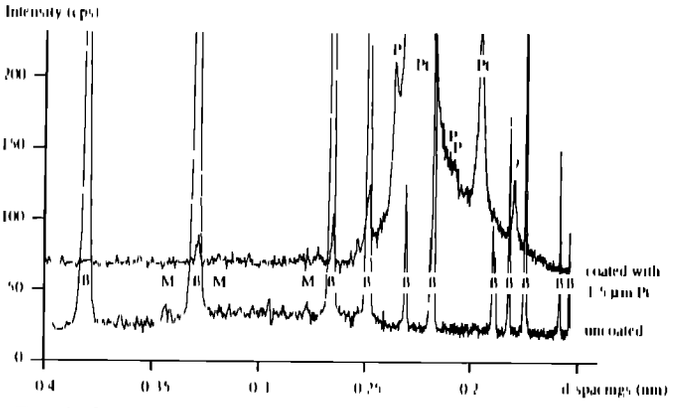

Fig. 1. XRD patterns of uncoated and 1.5 µm Pt coated material A in Bragg-Brentano geometry. B: β-Si_3N_4, P: Pt_3Si, M: $Y_2Si_3O_3N_4$

Table 1. Compositions and properties of the silicon nitride materials under study

Material	*Content (mass %)*			*Specimen size* (mm³)	*Mechanical treatment*	*Integral middle surface roughness* (R_a) (μm)	*Relative density* (%)	*Three point bending at room temperature* (σ_3) (MPa)	*Mass gain per surface unit* ($\Delta m/S$) *at 1300 °C 100 h* (mg/cm²)
	HfO_2	Nd_2O_3	Y_2O_3						
A	2.0		6.0	13 × 13 × 3	Polishing	0.01 ± 0.005	98		0.378 ± 0.010
B	4.0	4.1		3 × 4 × 30	Grinding	0.4 ± 0.02	99.4 ± 0.3	867 ± 30	0.485 ± 0.008

and FeK_α radiation [9]. For the phase analyses and the grazing incidence angle investigations a horizontal diffractometer with CuK_α radiation was used.

The specimens were oxidized by cyclical annealing in dry air with a flow rate of 20 litres/h at 1100 °C, 1300 °C and 1450 °C for a total time of up to 150 h. The test bars were placed on an Al_2O_3 plate in an alumina tube. Pt wires were used to prevent contacts between the alumina plate and specimens during oxidation. The bars were removed from the furnace after various time intervals and weighed with a microbalance capable of 10⁻⁵ g resolution. The oxidized specimens were characterized as before oxidation. For microstructural evaluation of the surface layer polished cross sections were examined.

For the separation of the influence of the oxidizing atmosphere from the influence of high temperature on the Pt surface layer, the specimens were annealed for up to 40 h at 1100 °C in flowing nitrogen. After different annealing times the surface of samples was analysed.

For identification of the various reactions and reaction temperatures thermogravimetric and differential thermal analysis (DTA/TG) together with differential scanning calorimetry (DSC) investigations were carried out in nitrogen and air up to 1500 °C with heating and cooling rates of 10 K/min (Al_2O_3 crucibles, specimen mass about 20 mg). For the same purpose high temperature XRD investigations were carried out in oxidizing atmosphere with a heating rate of 10 K/min up to 1200 °C. For these tests plates (3 × 4 × 0.5 mm³) were prepared from bars of material B and sputtered on both sides with 1000 nm Pt.

3 Results and Discussion

3.1 Characterization of the coatings

Optical and electron microprobe analyses of the coated specimens showed in all cases dense and coherent, fully closed Pt layers. The results of the roughness measurements before and after the Pt sputtering are shown in Table 2. The surface roughness of the ground specimens was slightly improved. In the range of measuring accuracy the roughness of the polished surfaces was not changed by coating and was independent from the Pt layer thickness.

The energy of Pt ions at the moment of the collision with the substrate surface under the sputtering conditions that were used was about 1–10 eV. Pushing and exciton processes in the substrate surface can lead to the formation of new phases during sputtering. Macroscopically, this energy addition results in increasing temperature up to 100 °C, measured at the substrate holder. XRD, stress analysis and thin film analysis were used to determine the formation of new compounds at the platinum/silicon nitride interface and to study any change in the platinum lattice constant as a function of the distance from the Si_3N_4 surface. The XRD patterns of the uncoated and Pt coated specimens of material A, measured in Bragg–Brentano geometry, are shown in Fig. 1. The pattern of the Pt coated surface shows apart from the peaks of β-Si_3N_4 and the peaks of cubic Pt additional peaks which belong to γ-Pt_3Si. After changing the measuring geometry from Bragg–Brentano into grazing X-ray incidence angles at incidence angles of $\omega = 10°$ new peaks appear at $d = 0.3046$ nm, 0.2681 nm, 0.2106 nm and 0.1784 nm. The peak at $d = 0.2681$ nm probably belongs to PtO. The other additional peaks cannot be related to a known phase. The appearance of Pt_3Si shows that sputtering processes may lead to the formation of new phases at the substrate/layer interface. Such formation of binary and ternary metal silicides as products of reactions between Si_3N_4 and metals has been reported. The formation of Pt silicides proceeds in the low temperature range 200–600 °C [8]. At a microscopic localized level this temperature can be reached during sputtering processes regardless of the lower macroscopic temperature of the sample holder. Experiments with Pt coated glasses confirmed that these processes depend on the sputtering conditions (working

Table 2. Surface roughness before and after sputtering

Roughness	*Uncoated surfaces*		*Pt coated surfaces*	
	Ground	*Polished*	*Ground*	*Polished*
R_a (μm)	0.4 ± 0.02	0.01 ± 0.005	0.29 ± 0.02	0.02 ± 0.01
$R_{z\,DIN}$ (μm)	2.6 ± 0.1	0.28 ± 0.02	1.95 ± 0.10	0.31 ± 0.01

power/working pressure). The formation of Pt silicides in Si_3N_4 ceramics was also dependent on power and pressure. The rise of the working energy from 100 to 1000 W leads to the increase of the silicides content.

The X-ray investigations of residual stresses were carried out using uncoated and coated samples of material A (Pt layers of 405 nm, 810 nm and 1500 nm thickness). For the determination of texture and residual stresses interferences of several lattice planes were investigated[9]. The elastic constants, necessary for the calculation of stresses, were estimated from the Young's modulus and the Poisson constant. Residual compressive stresses of about 50 MPa were detected on both uncoated ground and polished Si_3N_4 surfaces. The Pt layers were also under compressive stresses and showed a ‹111› fibre texture. This texture was sharp at lower layer thickness and weak for thick layers and after annealing in nitrogen (caused by recrystallization). For Pt layers of 405 to 810 nm thickness the compressive residual stresses were high (≈ 450 MPa). They could be originated for instance by grain growth mechanisms or ion bombardment and interstitial solution of Ar atoms during the sputtering process. For high layer thickness up to 1500 nm, produced by longer sputtering time, the stresses decreased to ≈ 220 MPa. After annealing of the specimen with 810 nm Pt layer in nitrogen (20 litres/h, 2 h at 1100°C) the residual *compressive* stress changed to ≈ 200 MPa *tensile* stress (apparent yield point $\sigma_{0,2}$ of Pt at 20°C is 88.3 MPa[10]). This is caused by the difference of thermal expansion coefficients of Pt and Si_3N_4 ($\alpha_{Si_3N_4} = 3 \cdot 10^{-6}\ K^{-1}$, $\alpha_{Pt} = 9 \cdot 10^{-6}\ K^{-1}$). In Pt layers, deposited by electron beam evaporation, tensile stresses were also observed. For the investigations with grazing incidence angle material A with a 1500 nm thick Pt layer and the diffraction planes (111), (331) and (422) were selected. By changing the X-ray grazing incidence angle ω the penetration depth of X-rays varies and it is possible to get information about depth dependent changes of crystalline phases, lattice parameters and residual stresses. The investigations were carried out with $\omega = 0.5$–$16°$. The lattice parameters a were calculated by using the positions of the centre of gravity of the peaks in accordance with the equation

$$a = d(h^2 + k^2 + l^2)^{1/2}$$

d is the lattice spacing.

The results showed no significant changes of σ and lattice parameters with penetration depths. Figure 2 shows the dependence of the relative lattice constant changes on the angle ψ between reflecting plane and specimen surface. Peaks strongly influenced by texture are marked by 't'. From the 'method of

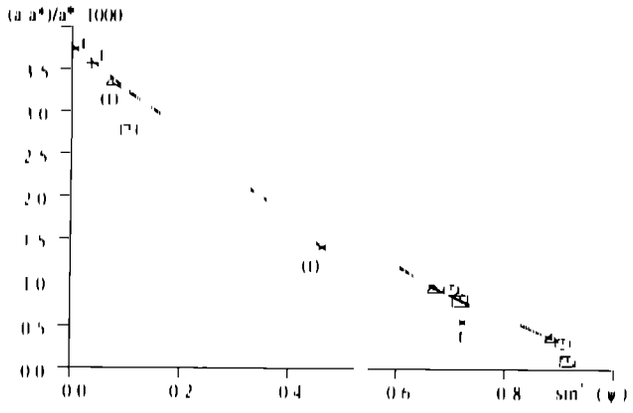

Fig. 2. Changes of Pt lattice constants a with $\sin^2(\psi)$ for various X-ray incidence angles ω: □, 1°; ○, 2°; △, 4°; +, 9°; ·, 16°; *t*, Peaks influenced by texture; a^*, 0.3923 nm, Pt lattice constant from Ref. 8

strain-free measuring direction'[11] for all investigated peaks a residual stress free Pt lattice constant of $a = 0.3927 \pm 0.0001$ nm was obtained, which is greater than the data published for Pt ($a_{Lit} = 0.39231$ nm[12]). The residual stretching of the Pt lattice should be caused by chemical effects (incorporation of Ar or Si into the Pt lattice). In the cubic face centred Pt lattice the large Ar atoms could occupy the $[\frac{1}{2}\,\frac{1}{2}\,\frac{1}{2}]$ places, while the Si could occupy the tetrahedral sites with the coordinates $[\frac{1}{4}\,\frac{1}{4}\,\frac{1}{4}]$. After annealing at 1100°C in nitrogen the stress free Pt/lattice constant decreased to $a = 0.3923 \pm 0.0001$ nm. The same value was obtained for a Pt layer of 1000 nm thickness produced by electron beam evaporation. The sputtering occurred in this case in vacuum (voltage 6 kV, vacuum 10^{-3} Pa). This supports the hypothesis that the changes of Pt lattice constant should be caused by incorporation of Ar.

3.2 Oxidation

The surface quality of the Pt coated specimen after high temperature exposure was better than that of the uncoated specimen. The Pt coating serves not as a protective layer in a direct way, because the specimen surfaces after high temperature exposition are not covered by a closed Pt coating (independent from the atmosphere) but by solidified melted structures (meandrous nets, drops), as shown in Fig. 3. The oxide layers on coated specimens show lower density and size of microcracks and bubbles and a higher crystallization degree (for Y or Nd silicates) than arises with uncoated specimens. The microcracks in the oxide scale are formed due to the β- to α transformation in cristobalite, whereas macrocracks and spalling of the oxide layer are a result of the volume expansion during the oxidation of Y or rare earth oxynitride crystalline phases, like melilite or wollastonite.[13] The change of the crack structure occurred in connection with a higher content of

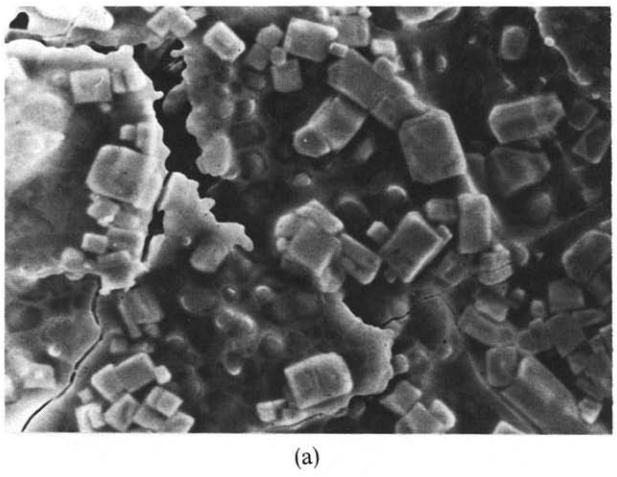

(a)

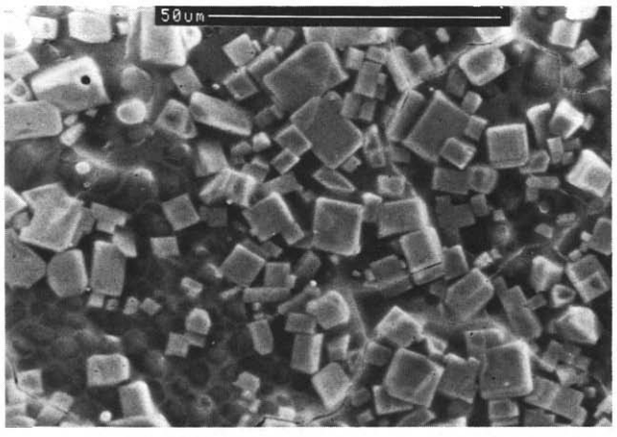

(b)

Fig. 3. Back scattered electron (BSE) images of specimen surfaces of material B after oxidation (1300 C, 100 h): (a) uncoated, (b) coated with 405 nm Pt.

$M_2Si_2O_7$ (M = Nd, Y) and a lower cristobalite content in the oxide layer of coated specimens. The ratio of integral intensity of the (101) γ cristobalite to the (008) A $Nd_2Si_2O_7$ XRD peaks and so the ratio of the amount of cristobalite to Nd silicate decreased after oxidation (1300 C, 100 h) from 0.25 (uncoated material B) to 0.15 (650 nm Pt sputtered material B). This leads to the supposition that the increase of oxidation resistance is caused by the change of crystallization mechanism and composition of the oxide layer. Table 3 shows the phase

Fig. 4. BSE image of 405 nm Pt coated surface of material A after oxidation at 1450 C, 12 h.

development of uncoated and coated specimens of material A before and after oxidation.

From the microscopic investigations it can be seen that the Pt structures that form during high temperature oxidation are associated with Y or Nd silicate crystals (Fig. 4). From the cross sections of the oxidized specimen one can see that most of the Pt drops lie at the outer surface of the oxide layer and are surrounded by grey crystalline silicates (Fig. 5). Pt was seldom found between the crystals, in the dark glassy phase. Such Pt drops sink through the glassy phase to the layer substrate interface.

Melting of Pt at low temperatures is caused by alloying with Si from the ceramic substrate during

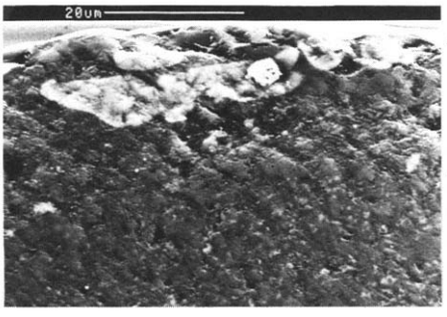

Fig. 5. BSE image of the polished cross section of material A coated with 810 nm Pt after oxidation at 1450 C, 12 h.

Table 3. Results of the XRD analyses of uncoated and with 810 nm Pt coated specimens of material A before and after oxidation

Before oxidation		*After oxidation*		
		at 1300 C, 100 h		at 1450 C, 100 h
Uncoated	*Coated*	*Uncoated*	*Coated*	*Coated*
β Si_3N_4	β Si_3N_4 Pt	β Si_3N_4	β Si_3N_4 Pt	β Si_3N_4 Pt
$Y_2Si_2O_3N_4$ ($Y_4Si_2O_7N_2$)	ε Pt_2Si PtO_2	α,β Cristobalite γ $Y_2Si_2O_7$ [a] α $Y_2Si_2O_7$	α,β Cristobalite β $Y_2Si_2O_7$ α $Y_2Si_2O_7$	α,β Cristobalite γ $Y_2Si_2O_7$ [a] β $Y_2Si_2O_7$

[a] 010 Texture

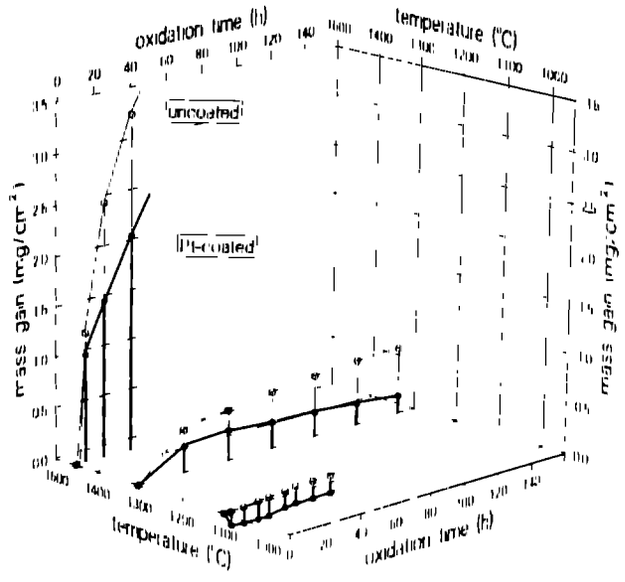

Fig. 6. Oxidation rate of uncoated and Pt coated polished material B versus temperature and time

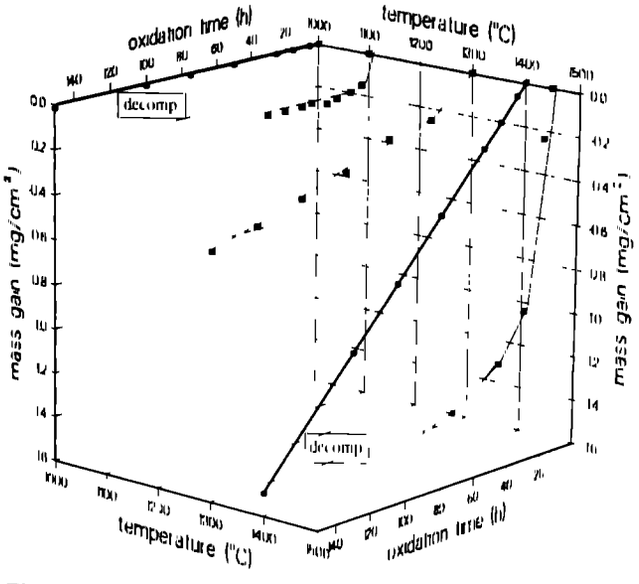

Fig. 7. Difference function from coated and uncoated material B versus oxidation temperature and theoretical decomposition function of platinum oxide ('decomp')

the sputtering process in accordance with the reaction

$$3\,Pt + 1\,Si_3N_4 \rightleftharpoons 2\,N_2 + 3\,Pt_3Si$$

Up to 1.4 at % Si can be dissolved in Pt. This leads to a reduction of melting temperature from 1769 °C to 830 °C, corresponding to the eutectic in the phase diagram Pt–Si between Pt and Pt_3Si [14]. An in situ inspection of the processes on 405 nm Pt coated surfaces (material A) with a high temperature microscope showed that melting and contracting of the Pt (or Pt silicides) occurred below 1000 °C. Melting of the silicides leads to a lower viscosity of the oxide layer and so to a change of the transport and crystallization processes in the layer.

The oxidation kinetics, i.e. the variation of the surface specific mass gain with time and temperature, were, in principle, the same for both materials. The oxidation kinetic curves for the uncoated and coated specimens of the material B obtained at 1100 °C, 1300 °C and 1450 °C are shown in Fig. 6. The uncoated material shows parabolic oxidation kinetics, which gives evidence of a diffusion controlled oxidation mechanism. For the coated specimens at all test temperatures a similar behaviour was observed: at the initial stage no significant (at low temperatures) or a little positive (at high temperatures) mass gain was detected and later a growing mass loss occurred.

Figure 7 shows the difference function that results from the difference $W'_{Pt}(t,T) - W(t,T)$ between the mass gain of coated $W'_{Pt}(t,T)$ and uncoated samples $W(t,T)$. This function is nearly linear with a change in gradient after the first 20 h. It contains the contributions of all occurring processes, except for the oxidation of uncoated silicon nitride, i.e. it also reflects any contribution from a change in the oxidation kinetics of silicon nitride itself. The mass loss during oxidation at 1100–1300 °C could be caused by the decomposition of a platinum oxide. The reaction between Pt and O_2 starts at 900 °C with the formation of the solid PtO_2. This oxide should be stable until about 1200 °C and should then decompose at higher temperatures. The mass loss in this case would be 0.0001 (0.01) mg/cm²/h in 48 litres/h flowing air at 1000 (1400) °C [15]. These rates of mass loss are given in Fig. 7 as 'decomp'. The real rates in the present case have to be smaller with increasing time because the reactive surface is reduced by the described melting and contracting of the Pt layer to form isolated structures. By use of a density $\rho_{Pt} = 21.4$ g/cm³ one gets for material B with 650 nm Pt a mass of the Pt layer of about 6 mg. According to Ref. 15 there would be no Pt at the surfaces after an oxidation time of about 7500 h at 1100 °C and 75 h at 1400 °C. Nevertheless, after oxidation at 1450 °C, 125 h some residual parts of Pt drops were found at the oxide layers (Fig. 4). This means that the differences of oxidation stability and oxidation kinetics between uncoated and coated samples cannot be explained only by the melting or decomposition of the Pt layer.

In order to investigate the influence of oxygen on the described processes coated specimens of material B were annealed at 1100 °C in nitrogen (dried, 20 litres/h, $t \geq 40$ h). No detectable mass loss was observed, but molten structures were built up from Pt at the surfaces. In contrast to the investigations with oxidizing atmosphere these structures show stronger isolated morphology like drops. Non isothermal DTA/TG—and DSC—investigations up to 1500 °C of 1000 nm Pt sputtered specimens of material B in nitrogen and in air did not lead to measurable thermal effects or mass changes. This can be caused by the fact that these processes relate

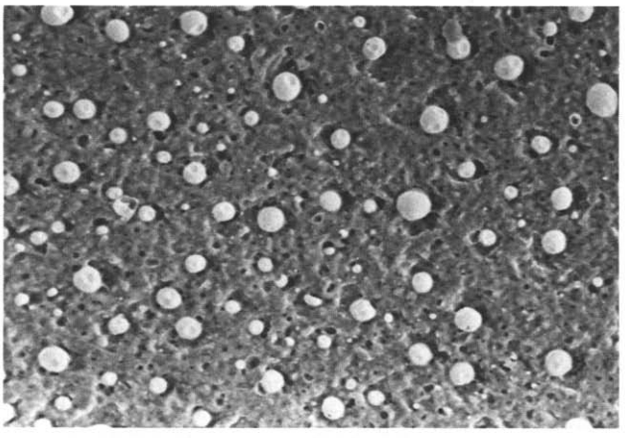

(a)

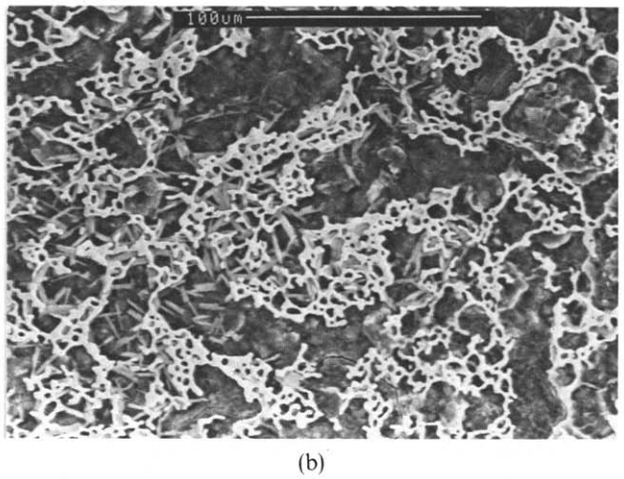

(b)

Fig. 8. BSE images of specimen surfaces of 1 µm Pt coated material B after nonisothermal annealing up to 1400 °C (a) in nitrogen (b) in dry air

to a very small volume and too small energy changes. Nevertheless the specimen surfaces showed the same appearance as after a long term oxidation or nitrogen annealing (Fig. 8).

High temperature XRD in air up to 1200 °C was used to show the phase development as a function of the temperature. Formation of crystalline phases could not be detected. Figure 9 shows diffraction patterns which were measured at 300 °C before and

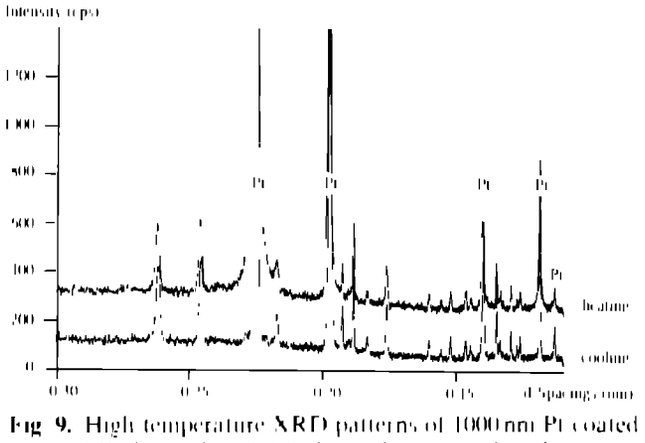

Fig. 9. High temperature XRD patterns of 1000 nm Pt coated material B obtained at 300 °C during heating and cooling in air (total heating was up to 1200 °C). Not marked peaks belong to β Si_3N_4

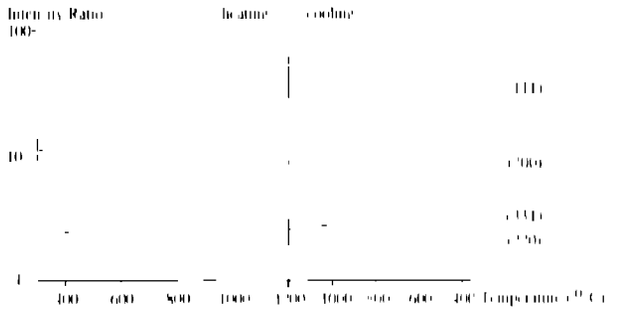

Fig. 10. Ratio of integral peak intensities of Pt reflecting planes to Si_3N_4 (301) in dependence from temperature. Material B coated with 1 µm Pt

after oxidation. Starting from about 800 °C the Pt peaks changed to sharp and higher contours. This could be caused by the healing of defects by stress relaxation and or by growth of the Pt crystals. Figure 10 shows the ratio of various Pt to Si_3N_4 (301) integral peak intensities as a function of temperature. The ratio increases with temperature up to about 800 °C, then decreases and remains during cooling at the lower level. The first part during heating, can be explained by the above mentioned causes. Above 800 °C the observed melting processes occur, connected with rearranging of the Pt crystals and weakening of the texture. The different degree of decrease of the peak intensity ratio is caused by the different influence on texture of the various reflecting planes.

4 Conclusions

The presence of Pt on the surfaces of dense silicon nitride improves its high temperature and long term stability in oxidizing atmosphere. The mechanism is associated at first with a separation of the ceramics surface from the oxidizing medium and later with a change in the composition, the phase development and the crystallization behaviour of the growing oxide layer, which includes a lower tendency to form cristobalite and a higher crystallization extent of Nd or Y silicates. This promotes the formation of an oxide layer with fewer and smaller cracks and bubbles.

Besides that the Pt silicides will also oxidize themselves, which can be described as like the oxidation of similar metal silicides,[16] by the decomposition of the Pt silicide into SiO and $PtSi_{y-1}$ or SiO and PtO, according to

$$PtSi_y + 0.5\,O_2 \rightleftharpoons xSiO + PtSi_{y-x}$$

$$PtSi_y + (1 + x/2)O_2 \rightleftharpoons xSiO + PtO_2$$

In this case Pt would serve as a transport medium for Si or SiO outwards and the oxide layer will become poor by Si or SiO. That leads to changes of

composition and of crystallization behaviour of the oxide layers.

The investigated minimal Pt layer thickness of 405 nm seems to be enough for changing the oxidation behaviour in the described way. Further investigations have to be done to provide a more complete understanding of the mechanism of the oxidation changes. The proposed method can be applied to improvement of the oxidation resistance of dense silicon nitride ceramics (in applications without abrasive wear) at temperatures above 1000 °C.

Acknowledgements

The authors wish to thank Dr G. Leitner (IKTS Dresden) for the DTA and DSC investigations, the colleagues from the Freiberger Präzisionsmechanik GmbH for their involvement in the XRD problems, Dr N. Mattern (IFW Dresden) for the high temperature XRD measurements and Dr D. Stephan (IFW Dresden) for valuable discussion.

References

1. Desmaison, J., High temperature oxidation protection coatings for monolithic or composite ceramics. *Werkstoffe und Korrosion*, **41** (1990) 749–50.
2. Wolf, G. K., Neue Anwendungen der Ionenstrahltechnik. *Ingenieur Werkstoffe*, **3**(12) (1991) 50–2.
3. Ballhause, P., Verschleißschutzschichten durch Sputter- und Ionenstrahltechnik. *Ingenieur Werkstoffe*, **3**(11) (1991) 56.
4. Klemm, H., Herrmann, M., Reich, T. & Hermel, W., High temperature properties of Si_3N_4 materials. *J. Eur. Ceram. Soc.*, **7** (1991) 315–18.
5. Liddell, K. & Thompson, D. P., X-Ray diffraction data for yttrium silicates. *Brit. Ceram. Trans. J.*, **85** (1986) 17–22.
6. Wolfstieg, U., ψ-Goniometer. *High Temp. Mater.* **31**(1–2) (1976) 19–22.
7. Schuster, J. C., Weitzer, F. & Bauer, J., Joining of silicon nitride ceramics to metals: the phase diagram base. *Mat. Sci. Eng. A* **105/106** (1988) 201–6.
8. Somiya, S., Mitomo, M., Yoshimura, M. (eds), *Silicon Nitride—1, Ceramic Research and Development in Japan*, Vol. 1 (1990) pp. 135–56.
9. Große, G., Taut, C. & Stephan, D., X-ray investigations of platinum layers on dense construction ceramics with regard to residual stresses and stressfree lattice constants. EPDIC II, Enschede 1992, in press.
10. Landoldt-Bornstein, 6th edn. No. IV 2b, Springer Verlag 1964, pp. 576.
11. Stephan, D. & Wetzig, K., Ausgezeichnete Meßrichtungen bei der röntgenografischen Spannungs- und Phasenanalyse an kompakten polykristallinen Proben. *Proc. 1. gemeins. Kristallographie Tagung*, München, 1991, p. 265.
12. ICPDS ICDD (c) 1990, 40802.
13. Gogotsi, Y. G. & Lavrenko, V. A., Corrosion of high performance ceramics. Springer Verlag, 1992.
14. Tanner, L. E. & Okamoto, H., The Pt–Si (platinum–silicon) system. *J. Phase Equilibria*, **12** (1991) 571–4.
15. Landoldt-Bornstein, 6th edn, No. IV, 2b. Springer Verlag, 1964, p. 626.
16. Stolt, L., Thomas, O. & d'Heurle, F. M., Oxidation of titanium, manganese, iron and niobium silicides: marker experiments. *J. Appl. Phys.*, **68**(10) (1990) 5133–9.